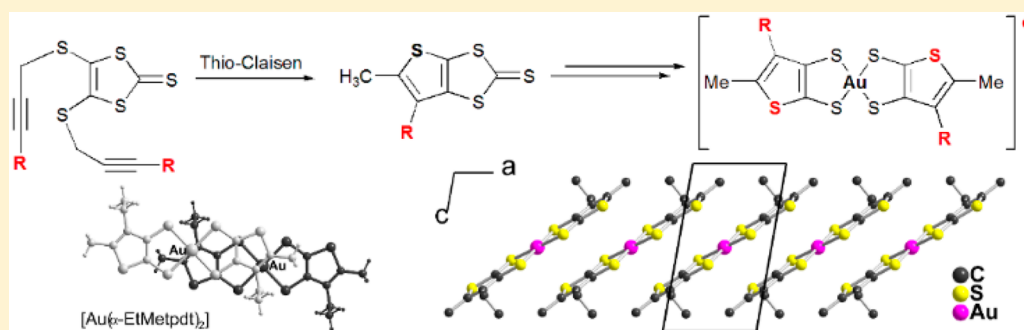


A Single-Component Conductor Based on a Radical Gold Dithiolene Complex with Alkyl-Substituted Thiophene-2,3-dithiolate Ligand

Toshiki Higashino,^{†,‡} Olivier Jeannin,[†] Tadashi Kawamoto,[‡] Dominique Lorcy,[†] Takehiko Mori,[‡] and Marc Fourmigué^{*,†}[†]Institut des Sciences Chimiques de Rennes (ISCR), Université Rennes 1, UMR CNRS 6226, Campus de Beaulieu, 35042 Rennes, France[‡]Department of Organic and Polymeric Materials, Tokyo Institute of Technology, O-okayama 2-12-1, Meguro-ku, 152-8552, Japan

Supporting Information



ABSTRACT: Alkyl-substituted thiophene-2,3-dithiolate ligands are prepared through a Thio-Claisen rearrangement of 4,5-bis(propargylthio)-1,3-dithiole-2-thione derivatives. The two novel dithiolate ligands, namely, 4,5-dimethyl-thiophene-2,3-dithiolate (α -Me₂tpdt) and 4-ethyl-5-methyl-thiophene-2,3-dithiolate (α -EtMe₂tpdt), are engaged in anionic Au(III) square planar complexes formulated as $[\text{Au}(\alpha\text{-Me}_2\text{tpdt})_2]^-$ and $[\text{Au}(\alpha\text{-EtMe}_2\text{tpdt})_2]^-$, isolated as Ph_4P^+ salts. Mono-electronic oxidation gives the neutral radical complexes $[\text{Au}(\alpha\text{-Me}_2\text{tpdt})_2]^\bullet$ and $[\text{Au}(\alpha\text{-EtMe}_2\text{tpdt})_2]^\bullet$. The latter crystallizes into uniform stacks with limited interstack interactions, giving rise to a calculated half-filled band structure. It exhibits a semiconducting behavior with room temperature conductivity of $3 \times 10^{-3} \text{ S cm}^{-1}$, indicating that this single-component conductor can be described as a Mott insulator. The different structures observed in $[\text{Au}(\alpha\text{-EtMe}_2\text{tpdt})_2]^\bullet$ and the known $[\text{Au}(\text{Et-thiazdt})_2]^\bullet$ complex (Et-thiazdt: N-ethyl-thiazoline-2-thione-4,5-dithiolate), despite their very similar shapes, are tentatively attributed to differences in the electronic structures of the ligand skeleton.

INTRODUCTION

Besides the well-known cation (or anion) radical organic salts investigated since the 1970s for their conducting (or even superconducting) properties,¹ single-component conductors based on one single neutral radical molecular entity have recently attracted much attention as they offer indeed the possibility for three-dimensional electronic structure, because of the absence of any counterion.² Also, while the stoichiometry is fixed by the ratio between electroactive molecule and counterion in mixed valence salts,³ doping strategies can be considered within single-component conductors, upon introduction of neutral, nonradical analogues.^{4,5} Besides the neutral tetrathiafulvalenedithiolate complexes developed by Kobayashi et al.,² neutral radical species provide another source of single-component conductors. One can distinguish purely organic species such as *spiro*-bis(phenalenyl)boron,⁶ bisdithiazolyl radicals,⁷ and catechol-conjugated tetrathiafulvalene (TTF) species,⁸ from neutral radical gold dithiolene complexes. The latter are formed from the $1e^-$ oxidation of the anionic, square planar d^8 Au^{III} dithiolene complexes $[\text{Au}(\text{dt})_2]^-$ to give

$[\text{Au}(\text{dt})_2]^\bullet$.⁹ Among the different complexes reported so far (Scheme 1), $[\text{Au}(\text{bdt})_2]^\bullet$ or $[\text{Au}(\text{F}_2\text{pdt})_2]^\bullet$ form uniform one-dimensional (1D) structures with semiconducting behavior,^{10,11} while $[\text{Au}(\text{dddt})_2]^\bullet$ associate into dimers with strong pairing of two radical species into the bonding combination of the two singly occupied molecular orbitals (SOMOs).¹² Higher conductivities were reported in $[\text{Au}(\alpha\text{-tpdt})_2]^\bullet$,¹³ or $[\text{Au}(\text{Et-thiazdt})_2]^\bullet$,¹⁴ with eventually transition to a metallic state under pressure, or under electric field pulses.¹⁵

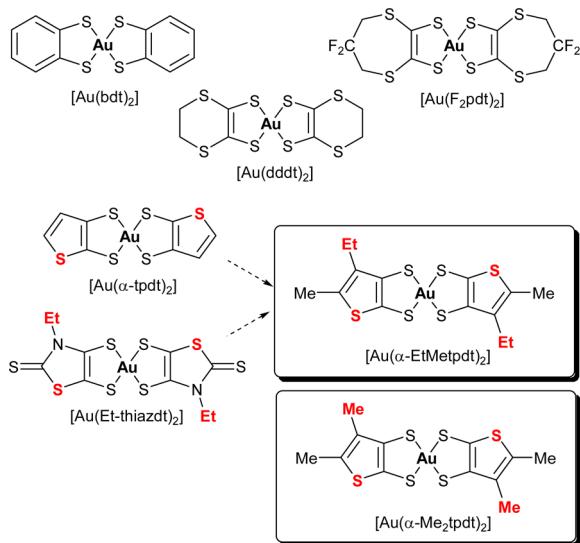
Considering the efficient two-dimensional (2D) packing adopted by $[\text{Au}(\text{Et-thiazdt})_2]^\bullet$,¹⁴ we wondered if an analogous structural motif possessing simultaneously the sulfur atom of the thiazoline (or a thiophene) ring and the ethyl substituent on the nitrogen atom could afford a similar solid state structure. For this purpose, we targeted the thiophene-2,3-dithiolate ligand (α -tpdt in Scheme 1),¹⁶ where the 4- at 5-positions can be substituted by alkyl groups, as in $[\text{Au}(\alpha\text{-EtMe}_2\text{tpdt})_2]^\bullet$ and

Received: July 24, 2015

Published: October 2, 2015



Scheme 1. Neutral Radical Gold Dithiolene Complexes

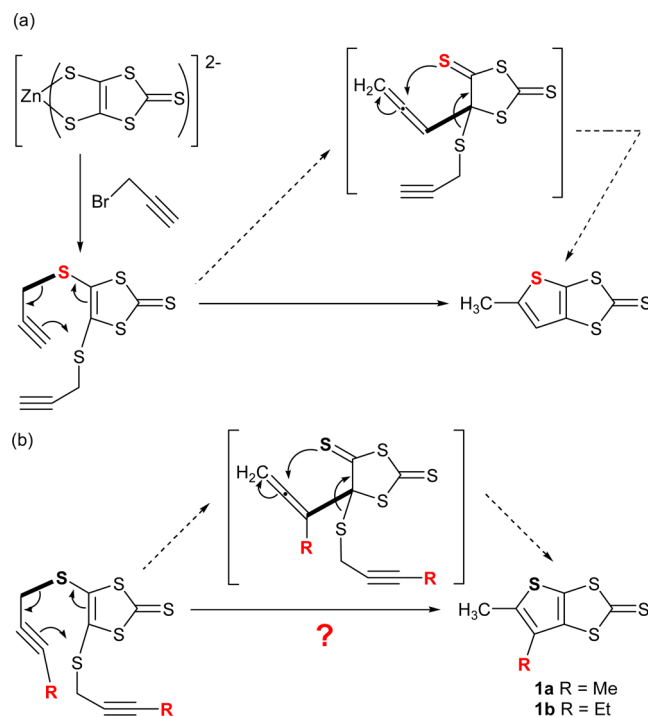


$[\text{Au}(\alpha\text{-Me}_2\text{tpdt})_2]^*$, the methyl group in 5-position mimicking the exocyclic thione in R-thiazdt, the alkyl group in 4-position mimicking the alkyl substituent on the nitrogen atom in R-thiazdt. We describe here the original synthesis of these two novel dithiolate ligands, the formation of the corresponding Au(III) bis-dithiolene anionic complexes and the successful electrocrystallization to the $[\text{Au}(\alpha\text{-EtMetpdt})_2]^*$ neutral radical, single-component conducting complex.

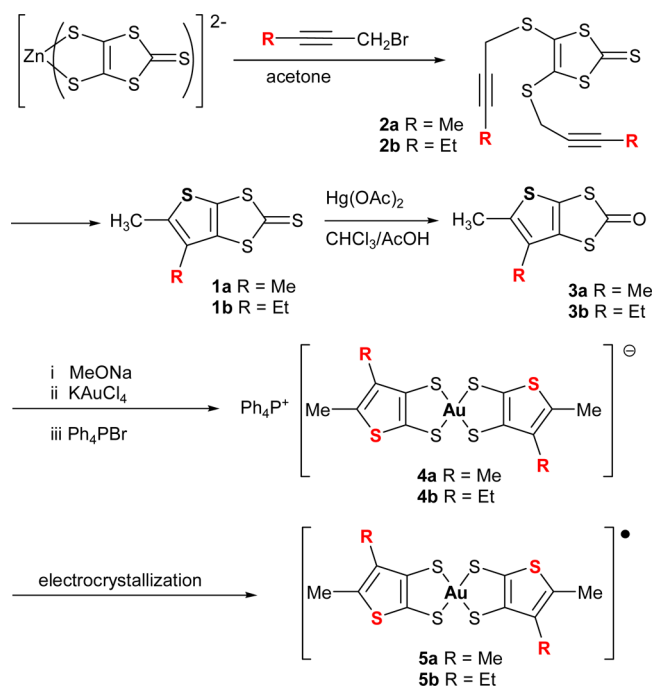
RESULTS AND DISCUSSION

The thiophene-2,3-dithiolate motif found in $[\text{Au}(\alpha\text{-tpdt})_2]$ has been reported by Almeida et al. from the aromatization of an hydrogenated precursor with 2,3-dichloro-5,6-dicyano-benzoquinone (DDQ), a synthetic procedure not easily extended to alkyl derivatives.^{13,17} Besides, he also reported a 5-methyl-substituted thiophene dithiolate precursor to give the corresponding gold complex $[\text{Au}(\alpha\text{-mtpdt})_2]^-$.¹⁸ This thiophene precursor, i.e., 5-methyl-1,3-dithiole-2-thione has been prepared from a bis-propargyl-functionalized dmit molecule (Scheme 2a), as described earlier by Singh et al.,¹⁹ through a Thio-Claisen rearrangement involving an allenic intermediate, in the presence of PPh_3 (Scheme 2a). On the basis of this reaction mechanism, we postulated (Scheme 2b) that the use of an alkyl-substituted propargyl bromide, such as $\text{Me-C}\equiv\text{C-CH}_2\text{Br}$ (1-bromo-2-butyne) or $\text{Et-C}\equiv\text{C-CH}_2\text{Br}$ (1-bromo-2-pentyne) will similarly afford the dithiole-2-thiones **1a** and **1b**, as precursors of respectively 4,5-dimethyl-thiophene-2,3-dithiolate ($\alpha\text{-Me}_2\text{tpdt}$) and 4-ethyl-5-methyl-thiophene-2,3-dithiolate ($\alpha\text{-EtMetpdt}$).

Indeed, the reaction of $(\text{Et}_4\text{N})_2[\text{Zn}(\text{dmit})_2]$ with 1-bromo-2-butyne or 1-bromo-2-pentyne (Scheme 3) gave the corresponding alkylpropargylthio-1,3-dithiole-2-thione derivatives, **2a** and **2b**, in respectively 98% and 89% yields. The cyclization in the presence of triphenylphosphine gave the corresponding 1,3-dithiole-2-thiones **1a** and **1b** in moderate yields, (28% for **1a** and 30% for **1b**), which were slightly better than those reported for the cyclization with the unsubstituted propargyl derivative (23%).¹⁹ The substitution scheme of the two trithiocarbonates **1a** and **1b** was also confirmed by single crystal X-ray diffraction (Figures S1 and S2 in Supporting Information). The following oxymercuration of **1a** and **1b** to

Scheme 2. (a) Proposed Mechanism for the Formation of 5-Methyl-1,3-dithiole-2-thione.¹⁹ (b) Extrapolation to 4-Alkyl-5-methyl Substituted Thiophene Derivatives **1a–b**

Scheme 3. Preparation of the Gold Dithiolene Complexes



the 1,3-dithiole-2-one derivatives afforded the pro-ligands **3a** and **3b** in respectively 97% and 82% yield.

The preparation of the anionic gold complexes was performed from **3a** and **3b** with MeONa, reaction with the Au(III) KAuCl_4 salt and cation metathesis with PPh_4Br to precipitate the two salts **4a** and **4b** in respectively 59 and 44%. Their electrochemical properties were studied by cyclic voltammetry (Figure S3 in Supporting Information). Both

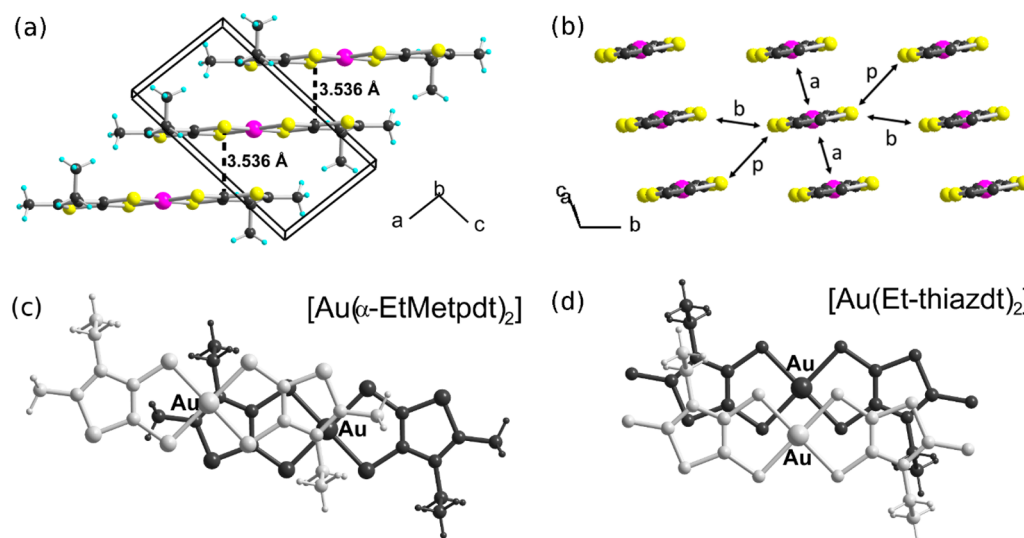


Figure 1. (a) View of the unit cell of **5b**. (b) View of one organic slab in **5b**, along the long molecular axis. Me and Et substituents were removed for clarity. Transfer integrals for the three SOMO–SOMO overlap interactions a, b, and p amount to 85.9, −1.80, and −18.2 meV respectively. (c) Overlap pattern within the chains in **5b**. (d) Overlap pattern in the reference complex $[\text{Au}(\text{Et-thiazdt})_2]$ (from ref 21).

complexes showed two quasi-reversible redox waves in dichloromethane solution. **4a** exhibits redox waves at $E_{1/2}^1 = -0.01$ V and $E_{1/2}^2 = +0.58$ V (vs. Ag/AgNO_3), corresponding to the oxidation process of $[\text{Au}(\alpha\text{-Me}_2\text{tpdt})_2]^- / [\text{Au}(\alpha\text{-Me}_2\text{tpdt})_2]^0$ and $[\text{Au}(\alpha\text{-Me}_2\text{tpdt})_2]^0 / [\text{Au}(\alpha\text{-Me}_2\text{tpdt})_2]^+$, respectively. Similarly, $[\text{Au}(\alpha\text{-EtMetpdt})_2]^-$ in **4b** shows almost the same redox potentials at $E_{1/2}^1 = 0.00$ V and $E_{1/2}^2 = +0.63$ V, corresponding to the oxidation from the monoanionic, to the neutral, and monocationic states. These $E_{1/2}^1$ values are lower than those reported for the 5-methyl-substituted thiophene derivative $[\text{Au}(\alpha\text{-mtpdt})_2]$ ($E_{1/2}^1 = 0.12$ V vs Ag/AgNO_3),¹⁸ illustrating the electron-releasing effect of the extra alkyl substituents. In general, the difference (ΔE) between $E_{1/2}^1$ and $E_{1/2}^2$ is a measure of the on-site Coulomb repulsion. In this case, these gold complexes show a ΔE value around 0.6 V, which is much larger than that found in the corresponding $[\text{Au}(\text{Et-thiazdt})_2]$ complex (0.13 V).¹⁴ Green-yellow crystals of **4a** and **4b** were obtained by recrystallization from acetone and investigated by single crystal X-ray diffraction. Both salts crystallize in the triclinic system, space group $P\bar{1}$, with a PPh_4^+ cation in general position, and two gold complexes, each of them on an inversion center, hence the 1:1 stoichiometry. Furthermore, one of the two crystallographically independent complexes in **4a** is disordered on two positions (Figure S4 in Supporting Information). Such a disorder was already encountered in $[\text{Ni}(\alpha\text{-mtpdt})_2]^0$, $[\text{Au}(\alpha\text{-mtpdt})_2]^-$,¹⁸ and $[\text{Ni}(\text{Me-thiazdt})_2]^-$ complexes,²⁰ while it does not affect the ethyl derivatives $[\text{Ni}(\text{Et-thiazdt})_2]^-$,²¹ $[\text{Au}(\text{Et-thiazdt})_2]^-$,^{14a} or $[\text{Au}(\alpha\text{-EtMetpdt})_2]^-$ in **4b** (Figure S5 in Supporting Information).

The neutral complexes **5a** and **5b** are easily obtained by chemical oxidation of the corresponding anions with iodine. The resulting dark green powders are soluble in DMF and DMSO, but recrystallization from these solvents does not afford any single crystals. The electrocrystallization of the monoanionic complex **4a** is also unsuccessful to give sufficiently large crystals suitable for X-ray measurements, probably because of a higher insolubility. On the other hand, the electrocrystallization of **4b** produces black plate-like crystals of **5b**, amenable to single-crystal X-ray structure analysis. It

crystallizes in the triclinic system, space group $P\bar{1}$, with one complex located on an inversion center, and therefore in a *trans* configuration. The radical complex is almost planar and forms a uniform stack along the *a*-axis with the interplanar spacing of 3.536 Å (Figure 1a,b), without any short S...S intermolecular contacts. The overlap between molecules along the chains is characterized indeed by a large displacement along the molecular long axis (Figure 1c), whereas $[\text{Au}(\text{Et-thiazdt})_2]^+$ having a similar molecular shape forms a θ -type packing with a small lateral offset (Figure 1d).

We have discussed earlier the possible origin of the different solid state associations, in the Et-thiazdt series, between the gold and nickel complexes, which differ only by the nature of the metal and the extra electron found in the gold complex.²¹ It was postulated that the overlap interaction between two radical complexes stabilized an almost eclipsed overlap in $[\text{Au}(\text{Et-thiazdt})_2]^+$, at variance with the closed shell $[\text{Ni}(\text{Et-thiazdt})_2]^0$ complexes where van der Waals contacts and π – π interactions favor a more compact shifted association, very similar to that observed here in **5b**. As illustrated in Figure 2, the frontier orbitals of the two radical complexes differ in several ways. We note indeed that in $[\text{Au}(\alpha\text{-EtMetpdt})_2]^+$ **5b**, the radical is more strongly localized on the metallacycles, while in the reference $[\text{Au}(\text{Et-thiazdt})_2]^+$ complex, it delocalizes extensively on the outer ends of the molecules and particularly the N and S

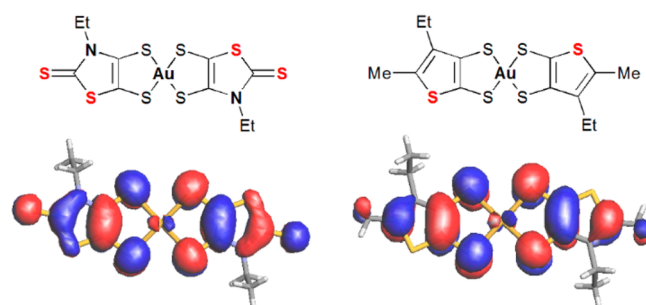


Figure 2. Details of the SOMO frontier orbital of the $[\text{Au}(\text{Et-thiazdt})_2]^+$ (left) and $[\text{Au}(\alpha\text{-EtMetpdt})_2]^+$ **5b** (right) complexes (drawn at the same 0.02 isocontour value).

heteroatoms of the thiazolinethione. As a consequence, the large longitudinal shift (Figure 1c) observed here between the radical $[\text{Au}(\alpha\text{-EtMetpdt})_2]^\bullet$ complexes in **5b** favors a more localized face-to-face interaction between S and C atoms of the metallacycles of two neighboring molecules. These differences also demonstrate that the rationalization of the exact stacking pattern of such π -type radical molecules is still a difficult task, at it is a compromise between π - π interactions (of quadrupolar nature), SOMO-SOMO overlap interactions and charge distribution within the molecules.^{22,23}

In order to investigate the electronic structure of **5b** in the crystalline state, the transfer integrals are estimated by the tight-binding band calculations.²⁴ Large transfer integrals are observed along the pseudostacking *a* axis, whereas the intercolumnar transfer integrals along *b* and *c* are small (see Figure 1b). These transfer integrals construct a 1D and half-filled band structure shown in Figure 3, since there is no HOMO-SOMO hybridization.

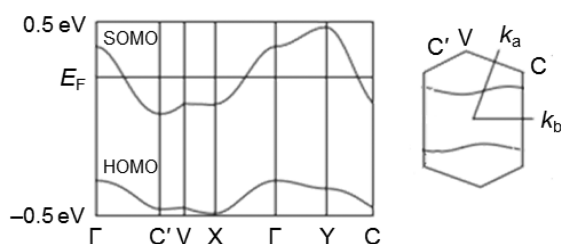


Figure 3. Calculated band structure for **5b** and associated Fermi surface (for a hypothetical metallic system).

Resistivity measurements were performed on a pellet sample of **5a**, and a single crystal of **5b**. They exhibit room-temperature conductivities of 0.01 S cm^{-1} and 0.003 S cm^{-1} , respectively, and an activated temperature dependence with the activation energy of 0.12 eV for **5a** and 0.15 eV for **5b** (Figure S5 in Supporting Information). In thermoelectric measurements, **5b** exhibits a large negative thermoelectric power of $-900 \mu\text{V K}^{-1}$ at room temperature (Figure S7 in Supporting Information), implying that the electrical conductivity is mainly mediated by electrons. Large thermoelectric power generally means highly correlated systems. The thermoelectric power shows very weak temperature dependence (Figure S7 in Supporting Information). With a decrease in the temperature, the absolute value of the thermoelectric power increases gradually with an activation energy of 0.93 eV, confirming the semiconductor-like behavior. Altogether, the transport properties and electronic structure with an half-filled band indicate that $[\text{Au}(\alpha\text{-EtMetpdt})_2]^\bullet$ **5b** can be described as a Mott insulator, with a strongly 1D character.

CONCLUSION

We have described here an efficient synthesis of alkyl-substituted thiophene dithiolate ligands based on a Thio-Claisen rearrangement, which can be easily extended to other propargyl derivatives. The formation of metal dithiolene complexes was illustrated through the formation of the corresponding gold dithiolene complexes. The electrocrystallization of the Au(III) $[\text{Au}(\alpha\text{-EtMetpdt})_2]^-$ anionic complex allowed for the isolation of the neutral $[\text{Au}(\alpha\text{-EtMetpdt})_2]^\bullet$, adding one more example to the very few structurally characterized single-component conductors based on such neutral radical gold complexes. It behaves as a Mott insulator

and is characterized by a large longitudinal shift between the interacting face-to-face radical complexes. The notable differences observed with the closely related $[\text{Au}(\text{Et-thiazdt})_2]^\bullet$ complex demonstrate that the solid state structures of such materials result from a very delicate balance between (i) the size, shape, and steric constraints which control the overall van der Waals contacts and π - π interactions, and (ii) the added stabilization brought by the overlap interaction between such radical complexes.²² This is particularly true within these gold dithiolene complexes where the SOMO is strongly delocalized on the two noninnocent ligands, with notable variations between the α -tpdt ligand with an aromatic thiophene ring and the R-thiazdt one, with a nonaromatic thiazoline-2-thione ring.

EXPERIMENTAL SECTION

General. Commercially available starting materials, such as 1-bromo-2-butyne and 1-bromo-2-pentyne, were used as received. The $(\text{TEA})_2[\text{Zn}(\text{dmit})_2]$ salt was prepared as previously described.²⁵ NMR spectra were recorded on a Bruker AV300III spectrometer at room temperature using perdeuterated solvents. Chemical shifts are reported in ppm referenced to TMS for ^1H NMR. Mass spectra were recorded at the Centre Régional de Mesures Physiques de l'Ouest, Rennes (France). Silica gel used in chromatographic separations was obtained from Acros Organics (Silica Gel, ultra pure, 40–60 μm).

Synthesis of 4,5-Bis(3-alkyl-prop-2-yn-1-ylthio)-1,3-dithiole-2-thione Derivatives 2. To a solution of tetraethylammonium bis(1,3-dithiole-2-thione-4,5-dithiol) zincate, $(\text{TEA})_2[\text{Zn}(\text{dmit})_2]$ (9.43 g, 10.0 mmol) in acetone (240 mL) was added dropwise 1-bromo-2-butyne (3.50 mL, 40.0 mmol) at 0 $^\circ\text{C}$, and the reaction mixture was stirred for 3 h at room temperature. The resulting suspension was filtered on Celite and washed with acetone. After the solvent was removed in vacuo, the crude product was purified by silica gel column chromatography (dichloromethane/petroleum ether 1:1, $R_f = 0.8$) to afford **2a** as an orange solid. Same procedure for **2b** starting from $(\text{TEA})_2[\text{Zn}(\text{dmit})_2]$ (3.20 g, 3.40 mmol) in acetone (120 mL) and 1-bromo-2-pentyne (1.39 mL, 13.6 mmol).

2a (5.95 g, 19.7 mmol, yield 98%) MS (EI) m/z 302 $[\text{M}]^+$; ^1H NMR (300 MHz, CDCl_3) δ 3.59 (q, $J = 2.4 \text{ Hz}$, 4H), 1.87 (t, $J = 2.4 \text{ Hz}$, 6H).

2b (2.00 g, 6.05 mmol, yield 89%) MS (EI) m/z 330 $[\text{M}]^+$; ^1H NMR (300 MHz, CDCl_3) δ 3.61 (t, $J = 2.4 \text{ Hz}$, 4H), 2.24 (tq, $J = 2.4 \text{ Hz}$, 7.5 Hz, 4H), 1.16 (t, $J = 7.5 \text{ Hz}$, 6H).

Synthesis of 5,6-Dialkylthieno[2,3-d][1,3]dithiole-2-thione derivatives 1. The mixture of **2a** (2.25 g, 7.44 mmol), triphenyl phosphine (7.80 g, 29.8 mmol) in toluene (100 mL) was refluxed for 16 h under Ar atmosphere. After the solvent was removed in vacuo, the crude product was purified by silica gel column chromatography eluted with hot petroleum ether and gradually added dichloromethane (dichloromethane/petroleum ether 1:1, $R_f = 0.4$). Initial colorless fractions ($R_f = 0.5$) yielded unreacted triphenyl phosphine. The resulting product was recrystallized from petroleum ether to afford **1a** as orange crystals. Same procedure for **1b** starting from **2b** (6.60 g, 20.0 mmol), triphenyl phosphine (15.7 g, 60.0 mmol) in toluene (300 mL).

1a (0.45 g, 2.1 mmol, yield 28%) MS (EI) m/z 218 $[\text{M}]^+$; ^1H NMR (300 MHz, CDCl_3) δ 2.46 (d, $J = 0.9 \text{ Hz}$, 3H), 2.16 (d, $J = 0.9 \text{ Hz}$, 3H).

1b (1.4 g, 6.0 mmol, yield 30%) MS (EI) m/z 232 $[\text{M}]^+$; ^1H NMR (300 MHz, CDCl_3) δ 2.57 (q, $J = 7.5 \text{ Hz}$, 2H), 2.47 (s, 3H), 1.19 (t, $J = 7.5 \text{ Hz}$, 3H).

Synthesis of 5,6-Dialkylthieno[2,3-d][1,3]dithiole-2-one Derivatives 3. To a solution of **1a** (1.00 g, 4.58 mmol) in a mixture of chloroform and acetic acid (100 mL, 3/2 v/v) was added mercury(II) diacetate (3.65 g, 11.4 mmol) at room temperature. After being stirred for 4 h, the white precipitate was filtered on Celite, and washed with dichloromethane. The filtrate was washed with distilled water, sodium hydrogen carbonate, and brine, dried over magnesium sulfate, and concentrated. The crude product was purified by silica gel column

Table 1. Crystallographic Data

	1a	1b	4a	4b	5b
formula	C ₇ H ₆ S ₄	C ₈ H ₆ S ₄	C ₃₆ H ₃₂ AuPS ₆	C ₃₈ H ₃₆ AuPS ₆	C ₁₄ H ₁₆ AuS ₆
formula weight	218.36	232.38	884.98	913.00	573.61
T (K)	298(2)	293(2)	298(2)	298(2)	293(2)
crystal system	monoclinic	monoclinic	triclinic	triclinic	triclinic
space group	<i>P</i> 2 ₁ / <i>c</i>	<i>P</i> 2 ₁ / <i>c</i>	<i>P</i> $\bar{1}$	<i>P</i> $\bar{1}$	<i>P</i> $\bar{1}$
<i>a</i> (Å)	8.442(3)	9.6042(3)	10.6373(5)	12.437(4)	6.08222(17)
<i>b</i> (Å)	10.174(2)	10.2419(4)	11.9558(19)	13.143(6)	7.4498(2)
<i>c</i> (Å)	10.579(3)	10.5970(4)	14.8591(6)	13.355(6)	10.5245(3)
α (deg)	90.00	90.00	101.7815(16)	62.31(3)	96.6635(18)
β (deg)	94.13(3)	102.974(5)	97.6679(13)	75.70(3)	97.3421(19)
γ (deg)	90.00	90.00	104.6311(12)	76.48(3)	109.1703(17)
<i>V</i> (Å ³)	906.2(5)	1015.77(6)	1755.5(3)	1855.0(13)	440.34(3)
<i>Z</i>	4	4	2	2	1
<i>D</i> _{calc} (g/cm ³)	1.600	1.520	1.674	1.634	2.163
Nb reflections (unique)	3097	24921	38540	12634	5133
Nb. unique	853	2325	8017	10838	1588
<i>R</i> _i	0.0606	0.0262	0.0635	0.0459	0.0716
<i>R</i> _w	0.2189	0.0747	0.1523	0.1261	0.1973
GOF	0.848	1.091	1.219	1.055	1.105

chromatography (dichloromethane/petroleum ether 1:1, *R*_f = 0.5), and recrystallization from methanol afforded **3a** as a white solid. Same procedure for **3b** starting from **1b** (0.55 g, 2.4 mmol) in a mixture of chloroform and acetic acid (50 mL, 3/2 v/v) with Hg(OAc)₂ (1.89 g, 5.92 mmol).

3a (0.90 g, 4.4 mmol, 97%) MS (EI) *m/z* 202 [M]⁺; ¹H NMR (300 MHz, CDCl₃) δ 2.44 (d, *J* = 0.6 Hz, 3H), 2.18 (d, *J* = 0.6 Hz, 3H).

3b (0.42 g, 1.9 mmol, 82%) MS (EI) *m/z* 216 [M]⁺; ¹H NMR (300 MHz, CDCl₃) δ 2.58 (q, *J* = 7.5 Hz, 2H), 2.45 (s, 3H), 1.18 (t, *J* = 7.5 Hz, 3H).

Synthesis of Tetraphenylphosphonium Salts of Gold(III) Bis(4,5-dialkyl-2,3-thiophene-dithiolate) 4. Sodium (0.46 g, 20 mmol) was added to dried methanol (10 mL) at 0 °C, and the mixture was stirred for 30 min under Ar atmosphere. After sodium was completely dissolved, the proligand **3a** (0.41 g, 2.0 mmol) was added to this solution of sodium methoxide in methanol, and the mixture was further stirred for 30 min. To the resulting yellow mixture was added dropwise a solution of potassium tetrachloroaurate (0.38 g, 1.0 mmol) in methanol (20 mL), which became a dark reddish brown solution. The inorganic precipitate was removed by filtration, and to the filtrate was added dropwise a solution of tetraphenylphosphonium bromide (0.42 g, 10 mmol) in methanol (6 mL). The resulting mixture was stirred overnight, and a greenish brown precipitate was formed. The solid was filtered and recrystallized from acetone to afford **4a** as a green-yellow plates. Same procedure for **4b** starting from Na (0.23 g, 10 mmol) in MeOH (10 mL), **3b** (0.25 g, 1.2 mmol), KAuCl₄ (0.22 g, 0.58 mmol) in MeOH (10 mL) and Ph₄PBr (0.24 g, 0.58 mmol) in MeOH (3 mL).

[PPh₄][Au(α-Me₂tpdt)₂] **4a** (0.52 g, 0.59 mmol, yield 59%) ¹H NMR (DMSO-*d*₆, 300 MHz) 7.96 (dt, *J* = 7.5, 2.1 Hz, 4H), 7.77 (m, 16H), 2.17 (s, 6H), 1.78 (s, 6H). Elemental analysis Calcd for C₃₆H₃₂AuPS₆: C, 48.86; H, 3.64. Found: C, 48.71; H, 3.28.

[PPh₄][Au(α-EtMetpdt)₂] **4b** (0.24 g, 0.26 mmol, yield 44%), green-yellow prisms. ¹H NMR (DMSO-*d*₆, 300 MHz) 7.97 (dt, *J* = 7.5, 2.1 Hz, 4H), 7.77 (m, 16H), 2.25 (q, *J* = 4.5 Hz, 4H), 2.19 (s, 6H), 0.98 (t, *J* = 4.5 Hz, 6H). Elemental analysis Calcd for C₃₈H₃₆AuPS₆: C, 49.99; H, 3.97. Found: C, 49.94; H, 3.71.

Synthesis of the Neutral Complex Gold Bis(4,5-dimethyl-2,3-thiophene-dithiolate) [Au(α-Me₂tpdt)₂] 5a. A solution of iodine (38 mg, 0.15 mmol) in acetone (6 mL) was added dropwise to a solution of **4a** (265 mg, 0.300 mmol) in acetone (60 mL). After stirring for 1 h, the resulting dark precipitate was filtered and washed with acetone to afford **5a** as a dark green powder (120 mg, 0.220 mmol, yield 73%).

Electrocrystallization. Crystals of [Au(α-Me₂tpdt)₂] **5a** or [Au(α-EtMetpdt)₂] **5b** were prepared electrochemically using a

standard H-shaped cell (15 mL) with Pt electrodes. An acetonitrile/ethanol (4/1) solution of [PPh₄][Au(α-Me₂tpdt)₂] (10 mg) or an acetonitrile solution of [PPh₄][Au(α-EtMetpdt)₂] (10 mg) was placed in the anodic compartment, and *n*-Bu₄NPF₆ (100 mg) was placed in both compartments. Black needles of [Au(α-EtMetpdt)₂] suitable for X-ray diffraction analysis were obtained on the anode upon application of a constant current 1.0 μA for 4 days at room temperature. On the other hand, black flake-like microcrystals of [Au(α-Me₂tpdt)₂] not suitable for X-ray diffraction analysis were obtained on the anode upon application of a constant current of 0.5 μA for 2 weeks at room temperature. In this case of [Au(α-Me₂tpdt)₂], other solvents (acetonitrile, dichloromethane, 1,1,2-trichloroethane, tetrahydrofuran, chlorobenzene, or anisole) afforded noncrystalline black solids.

Redox and Optical Properties. Cyclic voltammograms were measured on an ALS model 701E electrochemical analyzer in 0.1 M tetra-*n*-butylammonium hexafluorophosphate (*n*-Bu₄N⁺PF₆⁻) solutions of dichloromethane at a scan rate of 20, 50, and 100 mV/s. The reference electrode was Ag/AgNO₃ with a glassy carbon working electrode and a Pt supporting electrode.

Crystal Structures and Theoretical Calculations. The reflection data were collected, either on a Rigaku R-Axis RAPID-II diffractometer using CuKα X-ray from a rotating anode source with a confocal multilayer X-ray mirror (λ = 1.54187 Å), or on a APEXII Bruker-AXS diffractometer equipped with a CCD camera and a graphite-monochromated Mo Kα radiation source (λ = 0.71073 Å). Empirical absorption correction was applied with the ABSCOR program. The structures were solved by direct methods (SIR 2008) and refined by full-matrix least-squares by applying anisotropic temperature factors for all non-hydrogen atoms using the SHELX-97 programs.²⁶ The hydrogen atoms were placed at geometrically calculated positions. Details on crystallographic X-ray data collections and refinements are found in Table 1. The frontier orbitals (HOMO, LUMO) and intermolecular transfer integrals *t_i* were calculated on the basis of the extended Hückel molecular orbital calculations.

Transport Properties. The electrical resistivities were measured by the conventional four-probe method by using low-frequency alternating current (AC). The measurements were done along the crystal long axis, corresponding to the molecular stacking direction for **5b** (crystallographic *a* axis), in the temperature range from room temperature to 145 K for **5a** and to 240 K for **5b** under vacuum.

Thermoelectric Properties. The thermoelectric power was measured with two-terminal method in the temperature range from 290 to 335 K under He atmosphere, by sandwiching the crystal between two copper blocks.

■ ASSOCIATED CONTENT

■ Supporting Information

The Supporting Information is available free of charge on the ACS Publications website at DOI: 10.1021/acs.inorgchem.5b01678.

Figures S1–S7 (PDF)

X-ray crystallographic files (CIF)

■ AUTHOR INFORMATION

Corresponding Author

*E-mail: marc.fourmigue@univ-rennes1.fr.

Notes

The authors declare no competing financial interest.

■ ACKNOWLEDGMENTS

This work was made possible with financial support from ANR (France) under Contract No. ANR-12-BS07-0032, and from the international training program of the Japan Society for the Promotion of Science (JSPS).

■ REFERENCES

- (1) Batail, P. *Chem. Rev.* **2004**, *104*, 4887–4890.
- (2) (a) Tanaka, H.; Okano, Y.; Kobayashi, H.; Suzuki, W.; Kobayashi, A. *Science* **2001**, *291*, 285–287. (b) Kobayashi, A.; Fujiwara, E.; Kobayashi, H. *Chem. Rev.* **2004**, *104*, 5243–5264. (c) Kobayashi, H.; Kobayashi, A.; Tajima, H. *Chem. - Asian J.* **2011**, *6*, 1688–1704. (d) Cui, H.; Kobayashi, H.; Ishibashi, S.; Sasa, M.; Iwase, F.; Kato, R.; Kobayashi, A. *J. Am. Chem. Soc.* **2014**, *136*, 7619–7622.
- (3) For non-stoichiometric salts, see: Mori, T. *Chem. Rev.* **2004**, *104*, 4947–4970.
- (4) (a) Idobata, Y.; Zhou, B.; Kobayashi, A.; Kobayashi, J. *Am. Chem. Soc.* **2012**, *134*, 871–874. (b) Yasuzuka, S.; Idobata, Y.; Zhou, B.; Kobayashi, A.; Katoh, K.; Cui, H. B.; Kato, R.; Tokumoto, M.; Kobayashi, H. *J. Phys. Soc. Jpn.* **2014**, *83*, 074701(1–5). (c) Mebrouk, K.; Kaddour, W.; Auban-Senzier, P.; Pasquier, C.; Jeannin, O.; Camerel, F.; Fourmigué, M. *Inorg. Chem.* **2015**, *54*, 7454–7460.
- (5) Pal, S. K.; Bag, P.; Itkis, M. E.; Tham, F. S.; Haddon, R. C. *J. Am. Chem. Soc.* **2014**, *136*, 14738–14741.
- (6) (a) Mandal, S. K.; Samanta, S.; Itkis, M. E.; Jensen, D. W.; Reed, R. W.; Oakley, R. T.; Tham, F. S.; Donnadieu, B.; Haddon, R. C. *J. Am. Chem. Soc.* **2006**, *128*, 1982–1994. (b) Pal, S. K.; Itkis, M. E.; Tham, F. S.; Reed, R. W.; Oakley, R. T.; Haddon, R. C. *Science* **2005**, *309*, 281–284.
- (7) (a) Mailman, A.; Winter, S. M.; Yu, X.; Robertson, C. M.; Yong, W.; Tse, J. S.; Secco, R. A.; Liu, Z.; Dube, P. A.; Howard, J. A. K.; Oakley, R. T. *J. Am. Chem. Soc.* **2012**, *134*, 9886–9889. (b) Wong, J. W. L.; Mailman, A.; Lekin, K.; Winter, S. M.; Yong, W.; Zhao, J.; Garimella, S. V.; Tse, J. S.; Secco, R. A.; Desgreniers, S.; Ohishi, Y.; Borondics, F.; Oakley, R. T. *J. Am. Chem. Soc.* **2014**, *136*, 1070–1081.
- (8) (a) Isono, T.; Kamo, H.; Ueda, A.; Takahashi, K.; Nakao, A.; Kumai, R.; Nakao, H.; Kobayashi, K.; Murakami, Y.; Mori, H. *Nat. Commun.* **2013**, *4*, 1344(1–5). (b) Ueda, A.; Yamada, S.; Isono, T.; Kamo, H.; Nakao, A.; Kumai, R.; Nakao, H.; Murakami, Y.; Yamamoto, K.; Nishio, Y.; Mori, H. *J. Am. Chem. Soc.* **2014**, *136*, 12184–12192.
- (9) Kokatam, S.; Ray, K.; Pap, J.; Bill, E.; Geiger, W. E.; Le Suer, R. J.; Rieger, P. H.; Weyhermüller, T.; Neese, F.; Wieghardt, K. *Inorg. Chem.* **2007**, *46*, 1100–1111.
- (10) (a) Rindorf, G.; Thorup, N.; Bjørnholm, T.; Bechgaard, K. *Acta Crystallogr., Sect. C: Cryst. Struct. Commun.* **1990**, *46*, 1437–1439. (b) Schiødt, N. C.; Bjørnholm, T.; Bechgaard, K.; Neumeier, J. J.; Allgeier, C.; Jacobsen, C. S.; Thorup, N. *Phys. Rev. B: Condens. Matter Mater. Phys.* **1996**, *53*, 1773–1778.
- (11) Dautel, O. J.; Fourmigué, M.; Canadell, E.; Auban-Senzier, P. *Adv. Funct. Mater.* **2002**, *12*, 693–698.
- (12) Schultz, A. J.; Wang, H. H.; Soderholm, L. C.; Sifter, T. L.; Williams, J. M.; Bechgaard, K.; Whangbo, M.-H. *Inorg. Chem.* **1987**, *26*, 3757–3761.
- (13) Belo, D.; Alves, H.; Branco Lopes, E.; Duarte, M. T.; Gama, V.; Teves Henriques, R.; Almeida, M.; Perez-Benítez, A.; Rovira, C.; Veciana, J. *Chem. - Eur. J.* **2001**, *7*, 511–519.
- (14) (a) Tenn, N.; Bellec, N.; Jeannin, O.; Piekara-Sady, L.; Auban-Senzier, P.; Iniguez, J.; Canadell, E.; Lorcy, D. *J. Am. Chem. Soc.* **2009**, *131*, 16961–16974. (b) Yzambart, G.; Bellec, N.; Nasser, G.; Jeannin, O.; Roisnel, T.; Fourmigué, M.; Auban-Senzier, P.; Iniguez, J.; Canadell, E.; Lorcy, D. *J. Am. Chem. Soc.* **2012**, *134*, 17138–17148.
- (15) Stoliar, P.; Diener, P.; Tranchant, J.; Corraze, B.; Brière, B.; Ta-Phuoc, V.; Bellec, N.; Fourmigué, M.; Lorcy, D.; Janod, E.; Cario, L. *J. Phys. Chem. C* **2015**, *119*, 2983–2988.
- (16) Belo, D.; Almeida, M. *Coord. Chem. Rev.* **2010**, *254*, 1479–1492.
- (17) Silva, R. A. L.; Vieira, B. J. C.; Andrade, M. M.; Santos, I. C.; Rabaça, S.; Belo, D.; Almeida, M. *Beilstein J. Org. Chem.* **2015**, *11*, 628–637.
- (18) Neves, A. I. S.; Santos, I. C.; Coutinho, J. T.; Pereira, L. C. J.; Henriques, R. T.; Lopes, E. B.; Alves, H.; Almeida, M.; Belo, D. *Eur. J. Inorg. Chem.* **2014**, *2014*, 3989–3999.
- (19) Suresh Kumar, E. V. K.; Singh, J. D.; Singh, H. B.; Das, K.; Verghese, B. *Tetrahedron* **1997**, *53*, 11627–11644.
- (20) Eid, S.; Fourmigué, M.; Roisnel, T.; Lorcy, D. *Inorg. Chem.* **2007**, *46*, 10647–10654.
- (21) Filatre-Furcate, A.; Bellec, N.; Jeannin, O.; Auban-Senzier, P.; Fourmigué, M.; Vacher, A.; Lorcy, D. *Inorg. Chem.* **2014**, *53*, 8681–8690.
- (22) Fourmigué, M. In *The Importance of π -Interactions in Crystal Engineering*; John Wiley & Sons, Ltd.: Chichester, West Sussex, U.K., 2012; Chapter 6, pp 143–162.
- (23) Makedonas, C.; Mitsopoulou, C. A. *Eur. J. Inorg. Chem.* **2006**, *2006*, 590–598.
- (24) Mori, T.; Kobayashi, A.; Sasaki, Y.; Kobayashi, H.; Saito, G.; Inokuchi, H. *Bull. Chem. Soc. Jpn.* **1984**, *57*, 627–633.
- (25) Wang, C.; Batsanov, A. S.; Bryce, M. R.; Howard, J. A. K. *Synthesis* **1998**, 1615–1618.
- (26) (a) Burla, M. C.; Caliendo, R.; Camalli, M.; Carrozzini, B.; Cascarano, G. L.; de Caro, L.; Giacovazzo, C.; Polidori, G.; Siliqi, D.; Spagna, R. *J. Appl. Crystallogr.* **2007**, *40*, 609–613. (b) Sheldrick, G. M. *Acta Crystallogr., Sect. A: Found. Crystallogr.* **2008**, *64*, 112–122.